JOURNAL OF SOLID STATE CHEMISTRY 111, 357–364 (1994)

Study of $FePO_4$ Catalyst

M. M. Gadgil and S. K. Kulshreshtha[1]

Chemistry Division, Bhabha Atomic Research Centre, Bombay 400 085 India

Received May 5, 1993; in revised form October 4, 1993; accepted October 12, 1993

$FePO_4$ catalyst with and without Pd impregnation has been prepared and studied for its temperature induced crystallization and identification of the phases formed during hydrogen reduction using ^{57}Fe Mössbauer and XRD techniques. Amorphous $FePO_4$ transforms to a hexagonal form at ≈875 K. The reduction of amorphous $FePO_4$ takes place at ≈575 K and leads to the formation of $Fe_2P_2O_7$. The presence of palladium metal over ferric phosphate facilitates the reduction. Unlike amorphous $FePO_4$, reduction of crystalline $FePO_4$ takes place via the formation of an intermediate phase having δ = 1.15 mm/sec and ΔEq = 4.39 mm/sec. An ammonia adsorption–desorption study of $FePO_4$ catalyst reveals that both Brønsted and Lewis acid sites are present. The catalyst loses its Brønsted acid sites upon calcination at ≈875 K. During oxidative dehydrogenation of isobutyric acid to methacrylic acid, the amorphous $FePO_4$ catalyst is converted to $Fe_7(PO_4)_6$ and Pd metal facilitates this conversion.

INTRODUCTION

A large number of investigations have been carried out to study the physicochemical and catalytic properties of metal phosphates (1). Aluminum phosphate has been extensively investigated because of its relatively large surface area, thermal stability over a broad range of temperature, and surface acid–base characteristics (2–7). Iron orthophosphate, $FePO_4$, whose structure is isotypic with aluminum orthophosphate (berlinite) (8), has not been studied in detail for its physicochemical characteristics. In the past few years, iron phosphate has been used for oxidative dehydrogenation reactions (9, 10) because Fe cations can easily be reduced or oxidized, giving rise to a Fe^{3+}/Fe^{2+} redox couple. The study of noble metal impregnated iron phosphate will be of interest for such reactions due to its bifunctional behavior. This bifunctional character can arise due to the redox property of iron phosphate and the activation of reactants over noble metal centers which are supported on this phosphate. Keeping in mind this bifunctional property, we have investigated iron orthophosphate catalyst, with and without 2% palladium impregnation, for its physicochemical characteristics and the changes that occur during the catalytic conversion of isobutyric acid to methacrylic acid. In order to understand the mechanism of the catalytic process, it is desirable to identify various reduced phases formed during oxidative dehydrogenation reaction, but such studies are not available for $FePO_4$. We have systematically studied the reduction behavior of iron phosphate, with and without palladium metal impregnation, in flowing hydrogen at different temperatures and compared these reduced phases with those obtained during the catalytic conversion of isobutyric acid to methacrylic acid.

The existence of different types of acid–base sites on the surface of metal phosphates is responsible for the catalytic reactions (2–7). In oxidative dehydrogenation reactions, the product formation occurs via the consecutive homolytic abstraction of hydrogen from the adsorbed reactant intermediate (11). This abstraction of hydrogen is facilitated by the presence of Lewis acid sites, whose concentration mainly depends on the thermal treatment of the catalyst. Therefore, it is of interest to study the effect of calcination on the nature and strength of different types of acid sites present on the surface of the $FePO_4$ catalyst. In this communication, the results of ammonia adsorption–desorption, which give information about the number and nature of acid sites, are also reported for $FePO_4$ samples calcined at different temperatures.

EXPERIMENTAL

Iron phosphate was prepared from aqueous solutions of acidic ferric nitrate and diammonium hydrogen phosphate in stoichiometric ratio and was precipitated by slowly adding approximately 1 *M* solution of ammonium hydroxide at 295 K with constant stirring. The final pH of the solution was ≈7.5. The precipitate obtained was filtered and repeatedly washed with water and oven dried at 395 K for 24 hr. The precipitate was in the form of a gel containing approximately 30% water by weight. $FePO_4$ catalyst having approximately 2% Pd by weight was prepared by the wet impregnation method using $PdCl_2$ solution and oven dried ferric phosphate. To investigate the reduction behavior of the $Pd/FePO_4$ catalyst, the impreg-

[1] To whom correspondence should be addressed.

0022-4596/94 $6.00

nated sample was directly used, since $PdCl_2$ is reduced to Pd metal at much lower temperatures than the temperature at which $FePO_4$ reduction is initiated. For calcination studies, $Pd/FePO_4$ obtained by reduction of $PdCl_2/FePO_4$ at 375 K was used and the small amount of Fe^{2+} formed during the reduction process was converted back to the Fe^{3+} state during its subsequent heating in air. Parts of the oven dried $FePO_4$ and $Pd/FePO_4$ were simultaneously calcined at variable temperatures in air for 4 hr each in order to study the crystallization behavior of iron phosphate and the role of Pd metal.

The reduction behavior was studied by taking approximately 0.5-g samples of oven dried $FePO_4$ and $PdCl_2/FePO_4$ in two different segments of a quartz boat and heating them simultaneously in flowing hydrogen at different temperatures (every time fresh sample was taken) ranging from 375 to 875 K for a fixed duration of 2 hr. The samples were cooled to room temperature in hydrogen flow and taken out for characterization.

The ^{57}Fe Mössbauer spectra were recorded at room temperature, using a $^{57}Co/Rh$ source and a conventional constant acceleration spectrometer. By least-squares fitting, these spectra, the values of isomer shift (δ) (with respect to α-Fe at room temperature), and quadrupole splitting (ΔEq) were calculated.

Powder X-ray diffraction (XRD) patterns were recorded with nickel-filtered copper $K\alpha$ radiation (λ = 1.5418Å) with a scanning speed of 2° min^{-1} using a Philips powder diffractometer.

To study the ammonia adsorption–desorption characteristics, oven dried iron phosphate was placed in a quartz tube, plugged on both sides by quartz wool, calcined at different temperatures in flowing nitrogen for 4 hr to flush out the water vapors, and cooled to room temperature. Dry ammonia was passed over the iron phosphate sample at room temperature for about 1.5 hr so as to ensure a saturation composition of adsorbed ammonia. The excess ammonia was removed by flushing dry nitrogen at room temperature (for ≈3 hr). Adsorbed ammonia was desorbed by heating the sample at different temperatures in steps of 25 K, for a fixed duration of 1 hr each, under a flow of dry nitrogen gas. The desorbed ammonia was estimated by adsorbing it in 0.1 N H_2SO_4 and back titrating excess H_2SO_4 with 0.1 N NaOH.

To understand the changes occurring in the matrix of $FePO_4$ and $Pd/FePO_4$ catalysts during oxidative dehydrogenation of isobutyric acid to methacrylic acid, the spent catalyst was analyzed by XRD and ^{57}Fe Mössbauer spectroscopy. The catalytic reaction of isobutyric acid to methacrylic acid was carried out over a 0.5-g catalyst placed in a quartz tube. Vapors of isobutyric acid were passed over the catalyst at a particular temperature using nitrogen as a carrier gas. Oxygen in excess was also passed simultaneously over the catalyst. The unreacted isobutyric acid and the product formed were collected in a cold trap and analyzed by proton NMR. The reactions were carried out at different temperatures from 505 to 655 K by taking a fresh catalyst sample for every experiment.

RESULTS AND DISCUSSION

Calcination Behavior of Iron Phosphate

Figure 1 shows the representative ^{57}Fe Mössbauer spectra of iron phosphate recorded at room temperature after calcination at different temperatures. The oven dried sample shows a quadrupole doublet with isomeric shift δ = 0.37 mm/sec and quadrupole splitting ΔEq = 0.87 mm/sec. The observed linewidth (Γ = 0.55 mm/sec) has a slight excess and arises due to the amorphous nature of this sample, as seen from the X-ray diffraction results reported below. The spectrum remains almost identical up to a calcination temperature of 675 K, as can be seen from Fig. 1b. Calcination at higher temperatures leads to the decreased value of both the isomeric shift and the quadrupole splitting, as can be seen from Fig. 1c, where the representative spectrum of the sample calcined at 875 K is shown. These decreased values of the isomeric shift, δ = 0.27 mm/sec, and the quadrupole splitting, ΔEq = 0.67 mm/sec, obtained from the analysis of Fig. 1c, are in good agreement with those reported earlier for crystalline $FePO_4$ (12, 13). The observed linewidth for the calcined sample is found to be ≈0.39 mm/sec. The change in δ, ΔEq, and the Γ value arises due to the crystallization of amorphous $FePO_4$, as discussed below.

The X-ray diffraction study of oven dried iron phosphate samples calcined at different temperatures shows that up to 675 K it was amorphous and above that temperature a crystalline pattern was observed which is characteristic of anhydrous $FePO_4$ having a hexagonal structure.

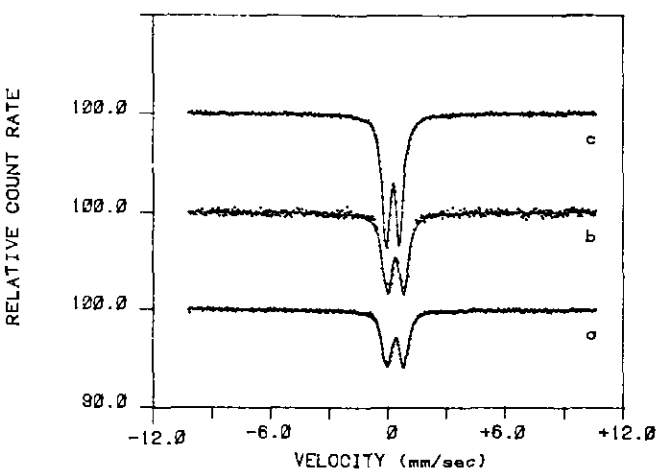

FIG. 1. ^{57}Fe Mössbauer spectra recorded at room temperature for $FePO_4$ precipitate calcined in air at (a) 395 K (oven dried), (b) 675 K, and (c) 875 K.

Figure 2 shows some of the representative X-ray diffraction patterns of $FePO_4$ samples calcined at different temperatures. The calcination behavior of the $FePO_4$ sample is not affected by Pd metal impregnation.

Reduction Behavior of $FePO_4$ and $Pd/FePO_4$

Figures 3 and 4 show the room temperature Mössbauer patterns of oven dried amorphous $FePO_4$ and $Pd/FePO_4$ reduced at various temperatures under hydrogen stream. From these figures, it can be seen that both Fe^{3+} and Fe^{2+} are present in varying ratios, depending on the reduction temperature. The isomer shift, the quadrupole splitting, and the fraction of Fe^{2+} obtained at different temperatures of reduction are listed in Table 1. Reduction of iron phosphate is initiated at 575 K (viz. Fig. 3d). At this stage, the values of δ and ΔEq of ferrous species are 1.16 and 2.57 mm/sec, respectively. On reduction at higher temperatures, the Fe^{3+}/Fe^{2+} ratio has decreased and complete reduction of Fe^{3+} state has taken place at 875 K (Fig. 3g). The ferrous species have an isomeric shift δ = 1.19 mm/sec and quadrupole spliting ΔEq = 2.42 mm/sec; these values are characteristic of $Fe_2P_2O_7$ (14). At this temperature of reduction, a part of the $Fe_2P_2O_7$ has also reduced to iron phosphides, FeP and Fe_2P, as seen from the central velocity region of the spectrum shown in Fig. 3g. The least-squares fitting of this spectrum gives the values δ = 0.26 mm/sec and ΔEq = 0.78 mm/sec for FeP. On the other hand, Fe_2P, which has two different Fe sites in equal ratio, has isomeric shift values δ = 0.32 and 0.59 mm/sec, with the corresponding values of quadrupole splitting ΔEq = 0.28 and 0.55 mm/sec, respectively. These values of δ and ΔEq are in good agreement with those reported in the literature (15).

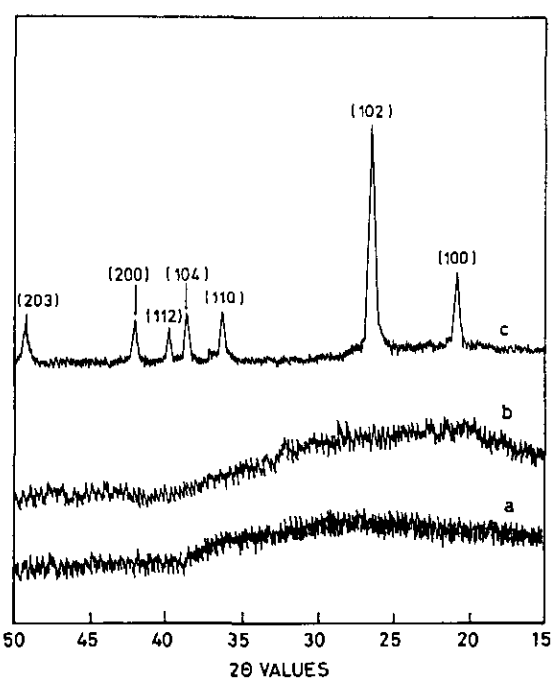

FIG. 2. XRD patterns of $FePO_4$ precipitate calcined in air at (a) 395 K (oven dried), (b) 675 K, and (c) 875 K.

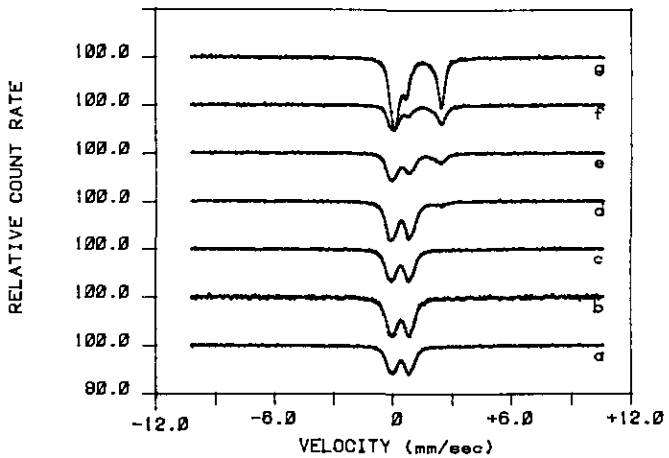

FIG. 3. ^{57}Fe Mössbauer spectra recorded at room temperature for amorphous $FePO_4$ heated in flowing hydrogen for 2 hr: (a) original sample, (b) at 375 K, (c) at 475 K, (d) at 575 K, (e) at 675 K, (f) at 775 K, and (g) at 875 K.

The reduction of $Pd/FePO_4$ is initiated at 375 K, showing the effect of the palladium impregnation. This indicates that the activation and spillover of hydrogen from Pd sites to the $FePO_4$ support has occurred. At this stage of reduction, the Mössbauer parameters obtained for Fe^{2+} are δ = 1.10 mm/sec and ΔEq = 2.64 mm/sec. Similar to the reduction of $FePO_4$, the $Pd/FePO_4$ sample also shows decrease in the value of quadrupole splitting upon increasing the reduction temperature. Reduction of $Pd/FePO_4$ at 775 K leads to the complete reduction of Fe^{3+} to the Fe^{2+} state and the Mössbauer parameters obtained

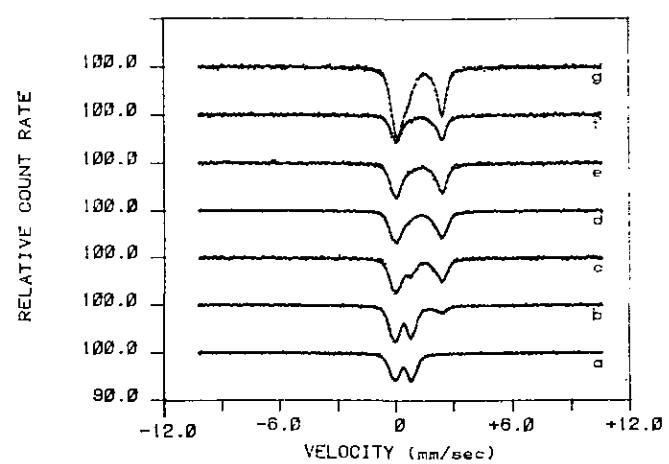

FIG. 4. ^{57}Fe Mössbauer spectra recorded at room temperature for palladium chloride impregnated amorphous $FePO_4$ heated in flowing hydrogen for 2 hr: (a) original sample, (b) at 375 K, (c) at 475 K, (d) at 575 K, (e) at 675 K, (f) at 775 K, and (g) at 875 K.

TABLE 1
Reduction in Flowing Hydrogen

Temperature of reduction (K)	Isomer shift δ (mm/sec)		Quadrupole splitting ΔEq (mm/sec)		Percentage of Fe^{2+} formed
	Fe^{3+}	Fe^{2+}	Fe^{3+}	Fe^{2+}	
$FePO_4$					
Original sample	0.37	—	0.87	—	—
375	0.37	—	0.87	—	—
475	0.36	—	0.90	—	—
575	0.47	1.16	0.69	2.57	5.1
675	0.40	1.10	0.81	2.57	30.9
775	0.45	1.17	0.60	2.48	71.4
875	—	1.19	—	2.42	59.8[a]
$Pd/FePO_4$					
375	0.39	1.07	0.81	2.64	16.3
475	0.44	1.11	0.62	2.46	65.7
575	0.38	1.15	0.39	2.41	85.4
675	0.35	1.17	0.43	2.40	93.6
775	—	1.21	—	2.38	100
875	—	1.20	—	2.40	62.8[a]

[a] The remaining fraction of iron is in the form of FeP and Fe_2P.

are $\delta = 1.21$ mm/sec and $\Delta Eq = 2.38$ mm/sec, which are similar to those obtained for $Fe_2P_2O_7$ during reduction of $FePO_4$. The small change in the values of the isomeric shift and quadrupole splitting for the $Fe_2P_2O_7$ phase may arise due to amorphous-to-crystalline phase transformation. The $Pd/FePO_4$ sample also shows partial conversion of $Fe_2P_2O_7$ to FeP and Fe_2P when reduced at 875 K, as seen from Fig. 4g.

X-ray diffraction study of reduced samples of $FePO_4$ and $Pd/FePO_4$ did not reveal any information up to the reduction temperatures of 675 and 575 K, respectively, as the samples are amorphous. $FePO_4$ reduced at 775 K, giving some indication about the formation of $Fe_2P_2O_7$ as indicated by the appearance of a Bragg reflection at $2\theta \approx 30.0$ (viz. Fig. 5b). The assignment of the Bragg reflections to $Fe_2P_2O_7$ is based on the XRD pattern of $Zn_2P_2O_7$, which is reported to be isostructural with $Fe_2P_2O_7$ (14). At this stage, even though reduction is not complete, as evidenced from the Mössbauer spectrum (Fig. 3f), $FePO_4$ reflections could not be seen in the XRD pattern because of $FePO_4$'s amorphous nature even after heating at 775 K. $Fe_2P_2O_7$ formation is clearly observed at 875 K, along with FeP and Fe_2P peaks indicating further reduction of $Fe_2P_2O_7$. The X-ray diffraction patterns of the samples obtained after reduction of $Pd/FePO_4$ at different temperatures (Figs. 5d–5g) are found to be essentially similar to those of $FePO_4$, but the process of reduction occurs at much lower temperatures and the relative yield of the different phases formed for a given temperature of reduction is found to be significantly different.

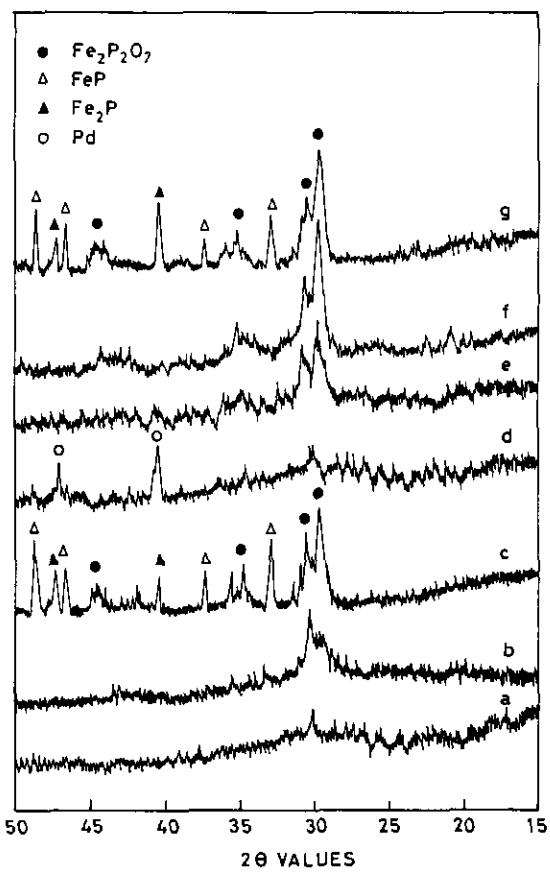

FIG. 5. XRD patterns of amorphous $FePO_4$ and $PdCl_2/FePO_4$ heated in flowing hydrogen for 2 hr as follows: $FePO_4$ heated at (a) 675 K, (b) 775 K, and (c) 875 K; $PdCl_2/FePO_4$ heated at (d) 575 K, (e) 675 K, (f) 775 K, and (g) 875 K.

To understand the crystallographic nature of the phases formed during reduction, the crystalline $FePO_4$ obtained by calcination of amorphous $FePO_4$ at 875 K for 4 hr in air is also investigated. The XRD patterns of samples reduced at different temperatures are shown in Fig. 6. It is observed that the crystalline iron phosphate is not reduced up to 675 K. Reduction is initiated at ≈725 K. At this stage of reduction, along with $FePO_4$ peaks, one extra peak is observed at $2\theta = 21.4$ ($d = 4.17$ Å) (Fig. 6b). At a still higher temperature of reduction (750 K), the intensity of this new peak has increased and two more extra peaks at $2\theta = 35.5$ ($d = 2.53$ Å) and $2\theta = 50.7$ ($d = 1.80$ Å) are also clearly seen (Fig. 6c). These Bragg reflections could not be assigned to any of the known phases of iron phosphates. Figure 6c also shows the formation of $Fe_2P_2O_7$. The unknown phase observed in the region 725–750 K has been termed an intermediate phase formed during reduction of crystalline iron phosphate, because on further reduction at 775 K, the intensity of this phase is decreased and it finally disappeared at 825 K, leaving behind only $Fe_2P_2O_7$ peaks (Fig. 6e). Unlike amorphous $FePO_4$, the crystalline $FePO_4$ does not show the formation of FeP and Fe_2P phases up to a reduction temperature of 875 K.

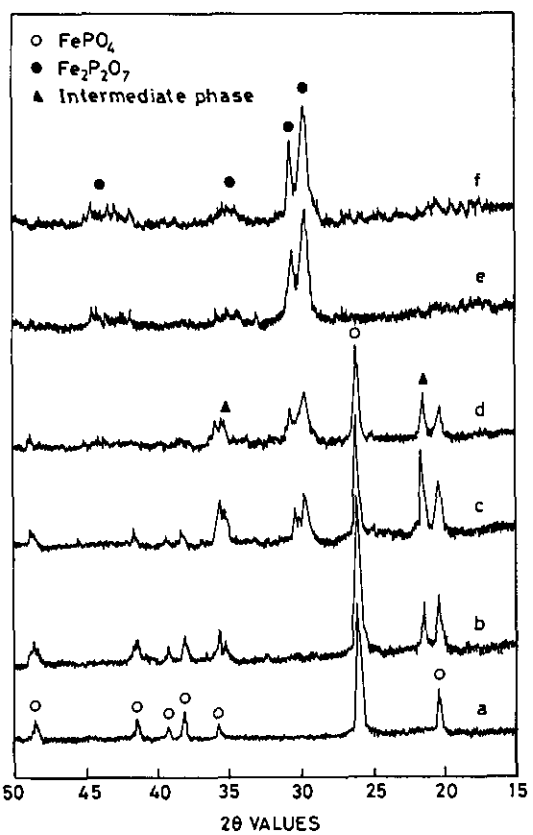

FIG. 6. XRD patterns of crystalline $FePO_4$ heated in flowing hydrogen for 2 hr at (a) 675 K, (b) 725 K, (c) 750 K, (d) 775 K, (e) 825 K, and (f) 875 K.

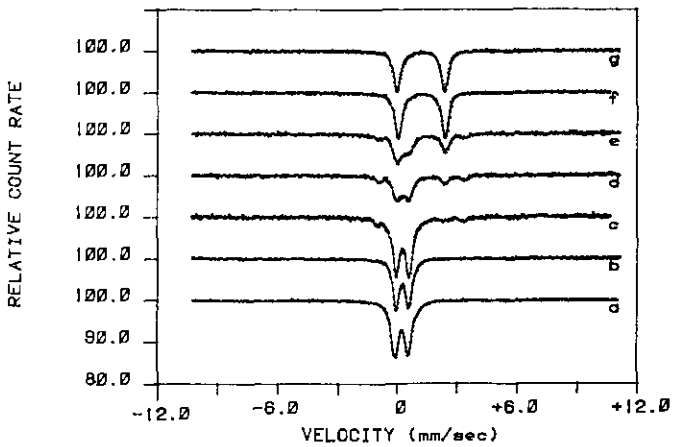

FIG. 7. ^{57}Fe Mössbauer spectra recorded at room temperature for crystalline $FePO_4$ heated in flowing hydrogen for 2 hr: (a) original sample, (b) at 675 K, (c) at 725 K, (d) at 750 K, (e) at 775 K, (f) at 825 K, and (g) at 875 K.

The reduced samples of crystalline $FePO_4$ are also characterized by ^{57}Fe Mössbauer spectroscopy and representative spectra are shown in Fig. 7. The Fe^{2+} ions present in the intermediate phase, which was observed in XRD pattern, show the isomer shift $\delta = 1.15$ mm/sec with very large quadrupole splitting $\Delta Eq = 4.39$ mm/sec, as seen from Figs. 7c–7e. The presence of Fe^{3+} ions in the intermediate phase cannot be ruled out from Mössbauer studies because of the existence of $FePO_4$, which is the major phase at this temperature of reduction. The variation of intensity of the intermediate phase as observed from the Mössbauer spectrum confirms the results obtained from the XRD pattern. Along with this intermediate, $Fe_2P_2O_7$ is also formed whose intensity increases with increasing temperature, and finally only $Fe_2P_2O_7$ is obtained. Mössbauer results of the sample reduced at 875 K do not show the formation of FeP or Fe_2P, which conforms with the XRD results.

Determination of Nature and Strength of Acid Sites

Figure 8 shows the plot of the amount of ammonia desorbed in mmole/g of $FePO_4$ catalyst as a function of temperature for samples precalcined at different temperatures. Ammonia is seen to desorb over a wide range of temperature and three characteristic peaks are observed for the sample calcined at 475 and 575 K. The first peak, having a maximum in the region of 350 to 375 K, is due to physisorbed ammonia on the surface (16), and the other two higher temperature peaks with maxima at 525 and 625 K are due to ammonia adsorption at acidic sites. The intensity of the peaks, and hence the total amount of ammonia desorbed, is found to decrease upon calcination at higher temperatures, showing reduction in acid sites. Ammonia is desorbed completely at 725 K irrespective

of calcination temperature. The ammonia desorption curve for 675 K calcined $FePO_4$ shows only one broad peak corresponding to adsorption at the acidic site having a maximum ≈625 K. This indicates that due to calcination of $FePO_4$ at 675 K, the adsorbed water, which is responsible for the formation of Brønsted acid sites, is removed and only the Lewis acid sites are left on the surface of $FePO_4$. From the above results, it is seen that the strength of the Lewis acid sites is more than that of the Brønsted acid sites on $FePO_4$.

Furthermore, the sample of $FePO_4$ saturated with adsorbed ammonia did not show any change in the values of the isomer shift and the quadrupole splitting, and also the diffraction pattern of the sample was not affected.

Modification in Catalyst during Oxidative Dehydrogenation Process

Mössbauer spectra of $FePO_4$ and $Pd/FePO_4$ spent catalysts are shown in Fig. 9. The spectra show that as the reaction temperature increases, the formation of Fe^{2+} also increases. Furthermore, reduction of Fe^{3+} to Fe^{2+} indicates that lattice oxygen is consumed in the reaction for the formation of methacrylic acid. The formation of methacrylic acid is confirmed from proton NMR spectra of the reaction product. However, the quantitative evaluation of the reaction products at variable temperatures of reaction could not be carried out because of the method of evaluation. The Mössbauer spectra also show that at a particular temperature of reaction, the relative fraction of Fe^{2+} formed was more for $Pd/FePO_4$ as compared to that for $FePO_4$. This indicates that palladium impregnation has facilitated the reaction. The values of Mössbauer parameters obtained from the fitting of these spectra are listed in Table 2 and suggest that during catalytic reation, $FePO_4$ has par-

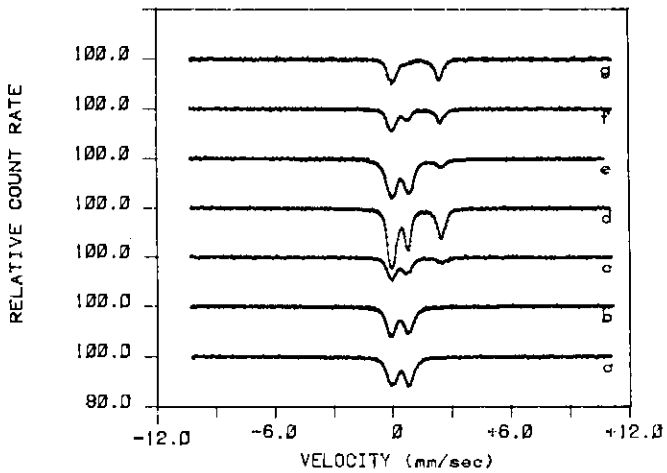

FIG. 9. ^{57}Fe Mössbauer spectra recorded at room temperature for $FePO_4$ and $Pd/FePO_4$ spent catalysts used for conversion of isobutyric acid to methacrylic acid at the following reaction temperatures for 4 hr: reaction over $FePO_4$ catalyst (a) original sample, (b) at 505 K, (c) at 555 K, and (d) at 655 K; reaction over $Pd/FePO_4$ catalyst (e) original sample, (f) at 505 K, and (g) at 655 K.

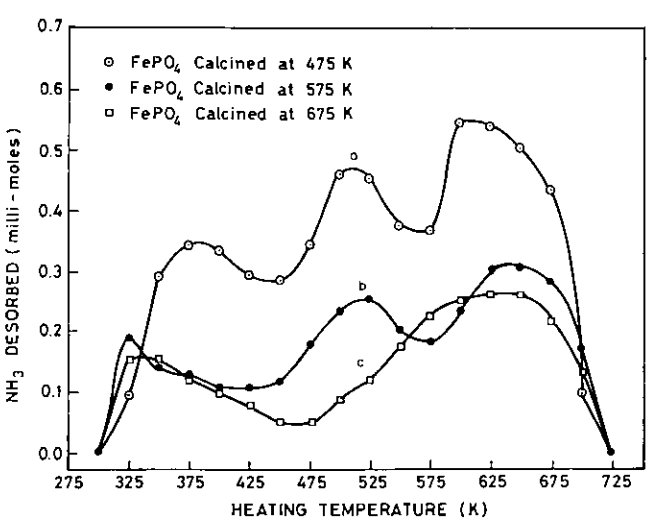

FIG. 8. Ammonia desorbed as a function of temperature from ammonia adsorbed $FePO_4$ catalyst precalcined at (a) 475 K, (b) 575 K, and (c) 675 K.

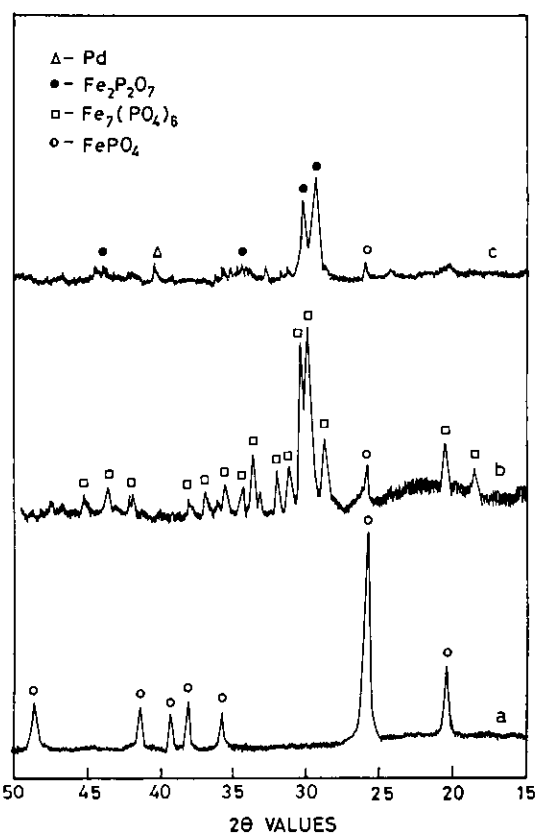

FIG. 10. XRD pattern of (a) crystalline $FePO_4$, (b) $FePO_4$ spent catalyst (reaction temperature 655 K), and (c) $Pd/FePO_4$ spent catalyst (reaction temperature 655 K).

TABLE 2
Mössbauer Parameters of Spent Catalyst

Temperature of reaction (K)	$FePO_4$		$Fe_7(PO_4)_6$		$Fe_2P_2O_7$		Percentage of Fe^{2+} formed
	δ (mm/sec)	ΔEq (mm/sec)	δ (mm/sec)	ΔEq (mm/sec)	δ (mm/sec)	ΔEq (mm/sec)	
$FePO_4$							
Before reaction	0.37	0.87	—	—	—	—	0.0
505	0.33	0.88	—	—	—	—	0.0
555	0.24	0.73	Fe^{2+} 1.20	2.63	—	—	24.0
			Fe^{3+} 0.45	0.74			
655	0.21	0.75	Fe^{2+} 1.17	2.62	—	—	41.0
			Fe^{3+} 0.42	0.73			
$Pd/FePO_4$							
Before reaction	0.34	0.86	Fe^{2+} 1.16	2.71	—	—	11.0
			Fe^{3+} 0.53	0.70			
505	—	—	Fe^{2+} 1.17	2.58	—	—	46.0
			Fe^{3+} 0.46	0.70			
655	0.29	0.85	—	—	1.20	2.37	84.0

tially transformed to $Fe_7(PO_4)_6$, which is confirmed by XRD results presented later in this section. On the other hand, when the catalytic reaction is carried out in the absence of oxygen, the spent catalyst shows the formation of $Fe_2P_2O_7$. This suggests that the oxygen in the feed gas mixture suppresses the complete reduction of $FePO_4$.

The representative XRD patterns of $FePO_4$ and $Pd/FePO_4$ spent catalysts are shown in Fig. 10 along with that of crystalline $FePO_4$ given for comparison. From these experiments, it is observed that $FePO_4$, which is initially in an amorphous state, becomes crystalline after catalytic conversion of isobutyric acid to methacrylic acid at 555 and 655 K reaction temperatures. The catalytic reactions at 555 and 655 K over $FePO_4$ have transformed the catalyst to mixed valence state iron phosphate, $Fe_7(PO_4)_6$ (ASTM 35-282), as seen from Fig. 10b, which corresponds to the catalyst used at 655 K. On the other hand, the $Pd/FePO_4$ catalyst used for this reaction at the same temperature shows transformation to the $Fe_2P_2O_7$ phase (Fig. 10c). This indicates that due to the presence of palladium over $FePO_4$, ferric to ferrous reduction is enhanced, which leads to the formation of $Fe_2P_2O_7$. The transformation of palladium impregnated $FePO_4$ to $Fe_7(PO_4)_6$ has occurred during this reaction at 505 K, as can be seen from the corresponding Fig. 9f and 9g, where a clear difference in the value of the quadrupole splitting of the Fe^{2+} species can be seen.

CONCLUSIONS

Oven dried amorphous $FePO_4$ crystallizes to a hexagonal form at ≈875 K. During the crystallization process, the values of the isomeric shift and the quadrupole splitting are reduced slightly.

The reduction of amorphous iron phosphate and palladium impregnated iron phosphate in hydrogen stream leads to the formation of $Fe_2P_2O_7$, which at higher temperatures of reduction is transformed to FeP and Fe_2P. Palladium accelerated the reduction rate as well as lowered the reduction temperature due to activation and spillover of hydrogen from metal centers to the support.

Crystallization of iron phosphate retards its reduction and makes a higher temperature necessary to initiate it. The pathway of reduction in crystalline iron phosphate is different from that of an amorphous one and proceeds via the formation of an unknown intermediate phase having large quadrupole splitting ΔEq = 4.39 mm/sec.

The ammonia adsorption–desorption study revealed the presence of both Brønsted and Lewis acid sites for samples calcined at temperatures lower than 575 K. The concentration of acid sites decreases upon calcination at higher temperatures due to the loss of the Brønsted acid sites.

The study of spent catalysts shows that during the catalytic transformation of isobutyric acid to methacrylic acid, $FePO_4$ is converted to $Fe_2P_2O_7$ through an intermediate mixed valence state $Fe_7(PO_4)_6$ phase. The presence of palladium on the catalyst enhances this reaction.

ACKNOWLEDGMENT

The authors are thankful to Dr. J. P. Mittal, Director of the Chemistry Group, for encouragement and very valuable suggestions.

REFERENCES

1. J. B. Moffat, *Catal. Rev. Sci. Eng.* **18,** 199 (1978).
2. J. Haber and U. Szybalska, *Faraday Discuss. Chem. Soc.* **72,** 263 (1981).
3. B. Gallace and J. B. Moffat, *J. Catal.* **76,** 182 (1982).

4. A. Schmidtmeyer and J. B. Moffat, *J. Catal.* **96,** 242 (1985).
5. S. F. Mitchell, G. Marcelin, and J. G. Goodwin, Jr., *J. Catal.* **105,** 521 (1987).
6. J. M. Campelo, A. Garcia, D. Luna, and J. M. Marinas, *J. Catal.* **111,** 106 (1988).
7. J. M. Campelo, A. Garcia, D. Luna, and J. M. Marinas, *J. Mater. Sci.* **25,** 2513 (1990).
8. H. N. Ng and C. Calvo, *Can. J. Chem.* **53,** 2064 (1975).
9. Ashland Oil Inc., C. Daniel *et al.,* U. S. Patent 4 298 755 (1981).
10. J. Mingzhi, C. Xianhao, X. Weiming, and L. Milang, *Hyp. Int.* **41,** 645 (1988).
11. O. Watzenberger, G. Emig, and D. T. Lynch, *J. Catal.* **124,** 247 (1990).
12. W. Meisel, J. Mintjens, and W. P. Bosman, *J. Phys. Chem. Solids* **49,** 157 (1988).
13. J. M. Millet, C. Virely, M. Forissier, P. Bussiere, and J. C. Vedrine, *Hyp. Int.* **46,** 619 (1989).
14. J. T. Hoggins, J. S. Swinnea, and H. Steinfink, *J. Solid State Chem.* **47,** 278 (1983).
15. R. Chandra, S. Bjarman, T. Ericsson, L. Haggstrom, C. Wilkinson, R. Wappling, Y. Andersson, and S. Rundqvist, *J. Solid State Chem.* **34,** 389 (1980).
16. Y. Chen, P. Wang, and W. Wang, *Catal. Lett.* **6,** 187 (1990).